Cell, Vol. 121, 207–221, April 22, 2005, Copyright ©2005 by Elsevier Inc. DOI 10.1016/j.cell.2005.04.004

microRNA-Directed Phasing during *Trans*-Acting siRNA Biogenesis in Plants

Edwards Allen,[1,2] Zhixin Xie,[1,2] Adam M. Gustafson,[1,2] and James C. Carrington[1,2,*]
[1]Center for Gene Research and Biotechnology
[2]Department of Botany and Plant Pathology
Oregon State University
Corvallis, Oregon 97331

Summary

Plants and animals use small RNAs (microRNAs [miRNAs] and siRNAs) as guides for posttranscriptional and epigenetic regulation. In plants, miRNAs and *trans*-acting (ta) siRNAs form through distinct biogenesis pathways, although they both interact with target transcripts and guide cleavage. An integrated approach to identify targets of *Arabidopsis thaliana* miRNAs and ta-siRNAs revealed several new classes of small RNA-regulated genes, including conventional genes such as Argonaute2 and an E2-ubiquitin conjugating enzyme. Surprisingly, five ta-siRNA-generating transcripts were identified as targets of miR173 or miR390. Rather than functioning as negative regulators, miR173- and miR390-guided cleavage was shown to set the 21-nucleotide phase for ta-siRNA precursor processing. These data support a model in which miRNA-guided formation of a 5′ or 3′ terminus within pre-ta-siRNA transcripts, followed by RDR6-dependent formation of dsRNA and Dicer-like processing, yields phased ta-siRNAs that negatively regulate other genes.

Introduction

microRNAs in plants and animals function as posttranscriptional negative regulators (Bartel, 2004; He and Hannon, 2004). Plant miRNAs target a disproportionately high number of genes with functions in developmental processes, including developmental timing, control of cell proliferation, meristem identity, and patterning. Global disruption of miRNA biogenesis or function, or disruption of specific miRNA-target interactions, generally results in developmental abnormalities (Achard et al., 2004; Chen, 2004; Emery et al., 2003; Juarez et al., 2004; Kidner and Martienssen, 2004; Laufs et al., 2004; Mallory et al., 2004; Palatnik et al., 2003; Tang et al., 2003; Vaucheret et al., 2004), indicating that miRNA-based regulation is integral to pathways governing growth and development.

Plant miRNAs usually contain near-perfect complementarity with target sites, which occur most commonly in protein-coding regions of mRNAs (Llave et al., 2002; Rhoades et al., 2002; Tang et al., 2003). As a result, most plant miRNAs function like siRNAs to guide target RNA cleavage (Jones-Rhoades and Bartel, 2004; Kasschau et al., 2003; Llave et al., 2002; Tang et al., 2003). In contrast, most animal miRNAs and possibly some plant miRNAs function to repress expression at the translational or cotranslational level (Ambros, 2003; Aukerman and Sakai, 2003; Chen, 2004; He and Hannon, 2004; Olsen and Ambros, 1999; Seggerson et al., 2002). Although many animal target mRNAs code for developmental control factors, no miRNAs or targets are conserved between plants and animals (Ambros, 2003; Bartel, 2004).

microRNAs form through nucleolytic maturation of genetically defined RNA precursors that adopt a self-complementary foldback structure. Processing yields a duplex intermediate (miRNA/miRNA*) that ultimately provides the miRNA strand to the effector complex, termed RISC (Khvorova et al., 2003; Schwarz et al., 2003). Plants contain four DICER-LIKE (DCL) proteins, one of which (DCL1) is necessary for maturation of most or all miRNA precursors (Kurihara and Watanabe, 2004; Park et al., 2002; Reinhart et al., 2002; Schauer et al., 2002). The DCL1 protein contains an RNA helicase and two RNaseIII-like domains, a central PAZ domain and C-terminal dsRNA binding motifs. HEN1 functions in miRNA biogenesis or stability by methylating the 3′ terminal residue (Yu et al., 2005). The dsRNA binding protein HYL1 is also necessary for miRNA biogenesis (Han et al., 2004; Liu et al., 2003; Pham et al., 2004; Tomari et al., 2004; Vazquez et al., 2004a). In animals, Exportin-5 (Exp5) regulates the transport of pre-miRNAs from the nucleus to the cytoplasm by a Ran-GTP-dependent mechanism (Bohnsack et al., 2004; Lund et al., 2003; Yi et al., 2003). In *Arabidopsis*, HASTY (HST) provides a related function for miRNA transport (Park et al., 2005). Active miRNA-containing RISC complexes in plants almost certainly contain one or more ARGONAUTE proteins, such as AGO1 (Fagard et al., 2000; Vaucheret et al., 2004). The mouse and human AGO2 proteins were shown to provide the catalytic activity within RISC complexes (Liu et al., 2004; Meister et al., 2004).

In addition to miRNAs, plants also produce diverse sets of endogenous siRNAs. These differ from miRNAs in that they arise from double-stranded RNA, which in some cases requires the activity of RNA-dependent RNA polymerases (RDRs). *Arabidopsis* DCL2, DCL3, RDR1, RDR2, and RDR6 have known roles in siRNA biogenesis (Dalmay et al., 2000; Mourrain et al., 2000; Peragine et al., 2004; Vazquez et al., 2004b; Xie et al., 2004; Yu et al., 2003). For example, DCL3 and RDR2 cooperate in the heterochromatin-associated RNAi pathway, resulting in 24-nucleotide siRNAs from various retroelements and transposons, ribosomal arrays, endogenous direct and inverted repeats, and transgenes containing direct repeats (Chan et al., 2004; Xie et al., 2004; Zilberman et al., 2003). RDR6 functions in post-transcriptional RNAi of sense transgenes, some viruses, and specific endogenous mRNAs that are targeted by *trans*-acting siRNAs (ta-siRNAs) (Dalmay et al., 2000; Mourrain et al., 2000; Parizotto et al., 2004; Peragine et al., 2004; Vazquez et al., 2004b; Yu et al., 2003). Ta-

*Correspondence: carrington@cgrb.oregonstate.edu

Table 1. *Arabidopsis* microRNA and ta-siRNA Target Families

Small RNA Family[a]	Target Family	Number of Targets	Target Function
microRNA			
miR156[b]	SBP[d,e,u]	11	transcription factor
miR158			
miR159[b]	MYB[d,f,g,u]	8	transcription factor
miR319[b]	TCP[g]	5	transcription factor
miR160[b]	ARF[d,e,u]	3	transcription factor
miR161[b]	PPR[d,h,u]	17	unknown
miR162[b]	DCL[i]	1	miRNA metabolism
miR163[b]	SAMT[h]	5	metabolism
miR164[b]	NAC[d,e,j,k,u]	6	transcription factor
miR166[b]	HD-ZIPIII[l,m,u]	5	transcription factor
miR167[b]	ARF[d,e,u]	2	transcription factor
miR168[b]	AGO1[d,n,u]	1	miRNA metabolism
miR169[b]	HAP2[r,u]	8	transcription factor
miR171[b]	SCR[d,o,u]	3	transcription factor
miR172[b]	AP2[e,p,q]	6	transcription factor
miR173	TAS1, TAS2[c]	4	ta-siRNA biogenesis
miR390	TAS3[c]	1	ta-siRNA biogenesis
miR393[b]	TIR1/F-box[r]	4	hormone signalling
	bHLH[r]	1	transcription factor
miR394[b]	F-box[r]	1	hormone signalling
miR395[b]	ATPS[r]	4	metabolism
	AST[c]	1	metabolism
miR396[b]	GRF[r]	7	transcription factor
miR397[b]	laccase/Cu oxidase[r]	3	metabolism
miR398[b]	CSD[r]	2	stress response
	CytC oxidase[r]	1	metabolism
miR399	E2-UBC[c]	1	ubiquitin conjugation
miR447	2PGK[c]	1	metabolism
miR403	AGO2[c]	1	miRNA metabolism
Trans-acting siRNA			
TAS1	Unclassified[s,t]	5	unknown
TAS2	PPR[c]	2	unknown
TAS3	ARF[c]	4	transcription factor

[a] Related miRNAs with up to five changes are grouped into a family.
[b] miRNAs with targets used in the rule development set.
[c] This target was validated only in this study.
[d] Vazquez et al. (2004a).
[e] Kasschau et al (2003).
[f] Achard et al. (2004).
[g] Palatnik et al. (2003).
[h] Allen et al. (2004).
[i] Xie et al. (2003).
[j] Mallory et al. (2004).
[k] Laufs et al. (2004).
[l] Tang et al. (2003).
[m] Emery et al. (2003).
[n] Vaucheret et al. (2004).
[o] Llave et al. (2002).
[p] Aukerman and Sakai (2003).
[q] Chen (2004).
[r] Jones-Rhoades and Bartel (2004).
[s] Vazquez et al. (2004b).
[t] Peragine et al. (2004).
[u] Rhoades et al. (2002).

siRNAs are genetically defined at specific loci and arise by phased, DICER-LIKE processing of dsRNA formed by RDR6/SGS3 activity on RNA polymerase II transcripts. Ta-siRNAs interact with target mRNAs and guide cleavage by the same mechanism as do plant miRNAs (Peragine et al., 2004; Vazquez et al., 2004b).

In this study, new *Arabidopsis* miRNA and ta-siRNA targets were identified through an integrated strategy that included computational, genome-wide expression profiling and experimental validation components. This revealed a surprising role for miRNAs in formation of ta-siRNAs in plants.

Results

Computational Prediction and Validation of New miRNA Targets

A rigorous set of computationally predicted and validated targets for most *Arabidopsis* miRNA families has emerged from several studies (Table 1 and see Table

S1 in the Supplemental Data available with this article online) (Aukerman and Sakai, 2003; Chen, 2004; Emery et al., 2003; Jones-Rhoades and Bartel, 2004; Kasschau et al., 2003; Llave et al., 2002; Mallory et al., 2004; Palatnik et al., 2003; Park et al., 2002; Rhoades et al., 2002; Tang et al., 2003; Vaucheret et al., 2004; Vazquez et al., 2004a; Xie et al., 2003). However, clear targets for several validated miRNAs (miR158, miR173, miR390/391, miR403, miR447) were not identified previously. To extend and refine the analysis of miRNA targets in plants, we developed a set of computational "rules" for *Arabidopsis* miRNA-target interactions involving 20 miRNA families. The rule development set included 55 previously published targets, 11 new validated targets, and 28 previously predicted targets that were closely related to validated family members. Ten of the 11 new validated targets were each from multigene families in which closely related paralogs were shown previously to be miRNA targets (Figure S1A). Characteristics used to define the rule set included position and frequency of miRNA-target mismatches, predicted stability of the miRNA-target duplex, and conservation of target sequences between orthologs in different species or between closely related paralogs within *Arabidopsis*. The miRNA-target mismatch rules were modified from those developed by Jones-Rhoades and Bartel (2004). MiRNA targets were predicted for both the *Arabidopsis* transcript database and the EST database, which provided increased opportunity to detect targets in nonannotated or misannotated genes. The complete methodology and supporting data for miRNA target prediction are provided in Supplemental Data.

A total of 109 targets was predicted, six of which were identified only in the EST search. Each predicted target was assigned to one of five bins (Figure 1A and Table S1). Bin 1 contained 63 of 66 previously validated targets that contributed to the rule set. Bin 2 contained 24 of the 28 predicted targets from the rule set. Thus, the overall false negative rate was 0.07. Bin 3 contained nine new predicted targets from existing target gene families. These included eight pentatricopeptide repeat (PPR) genes targeted by miR161.1 and miR161.2, and a HAP2a gene (At1g14020) targeted by miR169 (Figure S1B). Bin 4 contained nine targets from new families that were experimentally validated and analyzed in detail (see following sections). Experimental validation involved 5′RACE assays to detect a cleavage site opposite of position 10 from the 5′ end of the miRNA (Kasschau et al., 2003; Llave et al., 2002). Bin 5 contained four predicted targets that were tested but failed the 5′RACE validation assay. If Bin 5 genes represent all incorrect predictions from this search, then the false positive rate was 0.04.

Genes encoding an E2-ubiquitin-conjugating enzyme (E2-UBC, At2g33770), Argonaute2 (AGO2, At1g31280), a sulfate transporter (AST68, At5g10180), and a 2-phosphoglycerate kinase (2PGK, At5g60760) were validated as targets of miR399, miR403, miR395, and miR447, respectively, and represent the only conventional genes in Bin 4 (Figure 1B). The E2-UBC target, which was also predicted by Sunkar and Zhu (2004), contains five potential miR399-interacting sites in the 5′ untranslated region (UTR), although sites 2 and 3 appeared to be the predominant sites of miR399-guided cleavage (Figure 1B). The E2-UBC target mRNA joins TIR1, an E3 ligase targeted by miR393, as a second SCF complex-associated component under miRNA regulation (Jones-Rhoades and Bartel, 2004). The miR403 target site was identified within the 3′UTR of the AGO2 transcript from *Arabidopsis* and several other dicot families but not in orthologous transcripts from monocots. This is the second Argonaute family member identified as a miRNA target (Rhoades et al., 2002; Vaucheret et al., 2004). A function for AGO2 in either miRNA- or siRNA-guided processes is not yet known. MiR395 was previously validated to target the mRNA for an ATP sulfurylase, APS4, and to accumulate only in the presence of low levels of sulfate (Jones-Rhoades and Bartel, 2004). Interestingly, we identified and validated the mRNA for the sulfate transporter AST68 as a second miR395 target (Figure 1B). Both *APS1* and *AST68* are induced coordinately to promote sulfate uptake and utilization under low-sulfur conditions (Lappartient et al., 1999). This appears to be an unusual example of a plant miRNA regulating two independent gene families encoding proteins that function coordinately in the same metabolic pathway.

The five remaining genes in Bin 4 were validated as miR173 or miR390 targets (Figure 1C) and were predicted only from EST databases due to their unusual nature. These are discussed in detail below.

Expression Profiling of miRNA Targets

Most miRNAs of plants direct target cleavage. Loss-of-function mutations in miRNA metabolic or biogenesis genes, therefore, frequently result in elevated target transcript levels (Kasschau et al., 2003; Palatnik et al., 2003; Vazquez et al., 2004a; Xie et al., 2003). To systematically analyze the effects of miRNA and endogenous siRNA defects on validated and predicted miRNA target genes in *Arabidopsis*, expression profiling was done using nine mutant and two control plants. The mutants included miRNA-defective *dcl1-7*, *hen1-1*, and *hyl1-2* (Park et al., 2002; Schauer et al., 2002; Vazquez et al., 2004a), which were shown to reduce or eliminate accumulation of miRNAs, and a new insertion mutant, *hst-15*, with defects in nucleocytoplasmic transport of miRNA precursors (Park et al., 2005). In inflorescence tissue, *hst-15* had relatively modest effects on miRNA accumulation (Z.X., E.A., A. Calamar, and J.C.C., unpublished data). However, as shown using the *hst-1* mutant (Bollman et al., 2003; Peragine et al., 2004), *hst-15* had several developmental abnormalities, including a more rapid juvenile-to-adult phase transition, leaf curling and epinasty, altered silique phyllotaxy, and small flowers (Figure 2A). The mutant series also included five siRNA-defective mutants. The *dcl3-1* and *rdr2-1* mutants lack heterochromatin RNAi-associated siRNAs, *dcl2-1* and *rdr1-1* have defects in antiviral siRNA biogenesis, and *rdr6-15* is defective in ta-siRNA biogenesis (Peragine et al., 2004; Vazquez et al., 2004b; Xie et al., 2004; Yu et al., 2003). The *rdr6-15* mutant contains a new insertion allele but displays most of the same properties of previously characterized *rdr6* mutants (Peragine et al., 2004). Specifically, they display rapid juvenile-to-adult phase change and accompanying morphological defects (Figure 2A) and accumulate low levels of *rdr6-15* transcript (data not shown).

We predicted that miRNA target genes would be

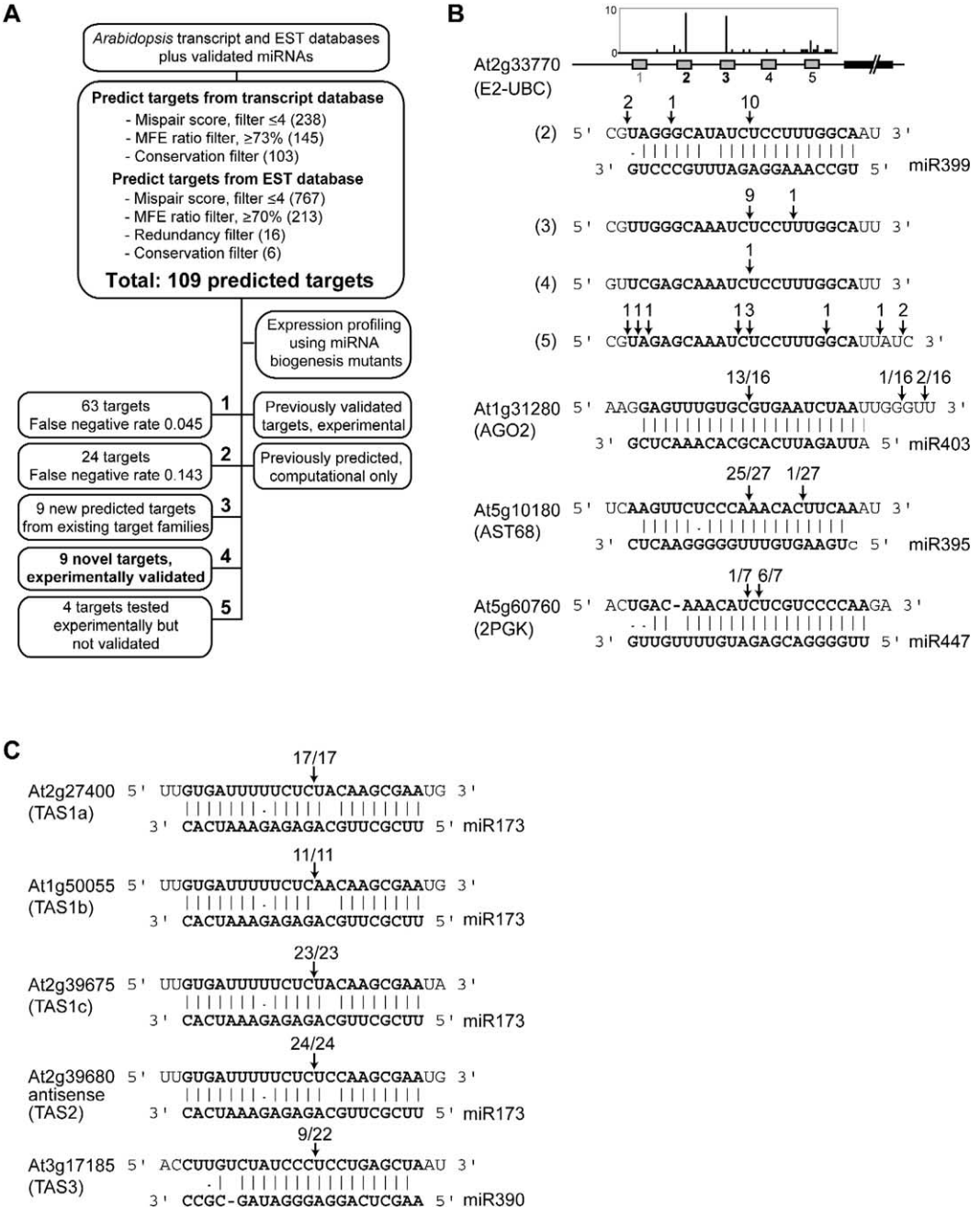

Figure 1. Prediction and Validation of *Arabidopsis* miRNA Targets

(A) Flowchart for miRNA target identification. The number of targets passing each step is shown in parentheses. Predicted targets were divided among five bins. The false negative rates in Bins 1 and 2 are based on 66 and 28 targets, respectively, in the rule development set. Validation of (B) protein-coding and (C) protein-noncoding miRNA targets by 5′RACE. Each miRNA-target duplex is highlighted, with the fraction of cloned, 5′RACE PCR products terminating at a given position indicated above the duplex. The distribution of cleavage products across all five predicted miR399 target sites is displayed above the schematic of At2g33770.

upregulated coordinately in *dcl1-7*, *hen1-1*, *hyl1-2*, and *hst-15* and largely unaffected in the siRNA biogenesis mutants. As a group, previously validated and predicted target genes (Bin 1+2 genes) generally behaved as predicted, although clearly not all genes were upregulated in the miRNA mutants (Figure 2B and Table S2). Of the 93 target genes present on the ATH1 array, 33 were significantly ($p < 0.01$, ANOVA) upregulated in two or more of the miRNA mutants. Targets from Bins 3+4, of which only 12 were represented on the array, were generally upregulated in the miRNA mutants but unaffected by the siRNA mutants, although the At2g39680 transcript (antisense to a validated miR173 target) was significantly upregulated in *rdr6-15* (Figure 2C). Five

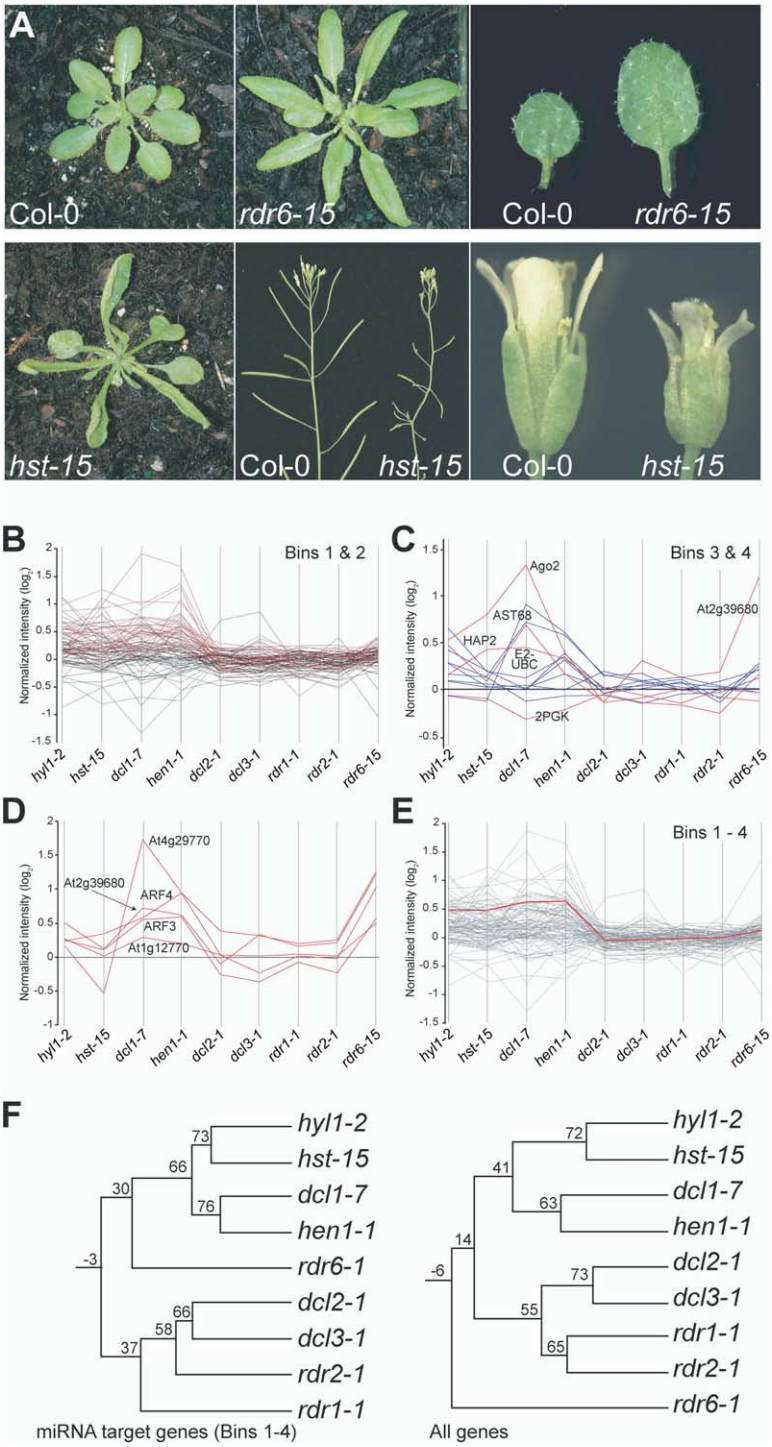

Figure 2. Characterization of *Arabidopsis* Small RNA Mutants

(A) Phenotype of *hst-15* and *rdr6-15* mutants. Rosette (Col-0, *rdr6-15*, *hst-15*), first true leaf (Col-0, *rdr6-15*), and bolt and flower (Col-0, *hst-15*) are shown. For microarray data (B–E), normalized intensity is plotted as $\log_2$ of fold change relative to the control sample for each mutant (zero represents no change in transcript abundance).

(B) Expression profile of 81 of 94 miRNA target transcripts that were predicted or validated previously and in this study (Bins 1 and 2). Transcripts that were upregulated (red) or downregulated (green) in *dcl1-7* are highlighted.

(C) Expression profile of 12 of 18 miRNA targets predicted in this study. Blue, new targets from existing target families (Bin 3); orange, novel miRNA targets (Bin 4).

(D) Expression profile of transcripts that were significantly coaffected ($p < 0.01$) in *dcl1-7*, *hen1-1*, and *rdr6-15*.

(E) Expression profile of 93 predicted or validated miRNA target transcripts (gray) and PCA component 1 (red).

(F) Cladogram of the small RNA biogenesis mutant series. The correlation among groups ($r \times 100$) is shown at each node.

genes, including At4g29770, At2g39680, At5g60450 (*Auxin Response Factor4*, *ARF4*), At2g33860 (*ARF3*), and At1g12770 were significantly upregulated ($p < 0.01$, ANOVA) in each of *dcl1-7*, *hen1-1*, and *rdr6-15* plants (Figure 2D). Transcripts for four of these (At4g29770, At1g12770, ARF3, and ARF4) were predicted or validated as ta-siRNA targets, and one (At2g39680) was a new type of miRNA target (see below).

A principal components analysis (PCA) was done to analyze variation patterns among all predicted and validated miRNA targets using expression data for genes in Bins 1–4. An eigenvector that accounted for 65% of the variation among conditions revealed that the miRNA mutants were unified by having target upregulation effects (Figure 2E). The siRNA mutants were unified by having no detectable effects (Figure 2E). No other eigenvector accounted for more than 9% of the variation. Among genes that were highly corre-

lated (r > 0.95) to the primary eigenvector was a 2PGK gene (At3g45090). This gene is closely related to the validated miR447 target gene but failed to meet the miRNA-target interaction criteria in the prediction algorithm. Additionally, unsupervised hierarchical clustering analyses were done using miRNA targets or all genes represented on the microarray. Correlated conditions were displayed using expression trees. Using both gene sets, the four miRNA-defective mutants grouped within one clade, with *dcl1-7/hen1-1* and *hst-15/hyl1-2* forming distinct subclades (Figure 2F). The siRNA-affected *dcl2-1*, *dcl3-1*, *rdr1-1*, and *rdr2-1* mutants formed a distinct expression clade using both gene sets (Figure 2F). Thus, with the major exceptions described below, the expression profiling data indicate that miRNA-mediated regulation of targets and downstream genes is largely independent of the siRNA-directed pathways.

miR173 Guides In-Phase Processing of Four ta-siRNA Primary Transcripts

Four miR173 targets were predicted from searches of the EST database. One of these predicted targets was antisense relative to the annotated gene At2g39680. Two other target sites were predicted within EST sequences AU235820 and CD534192 from two paralogous loci, which led to identification of a putative target site within a third paralogous locus (At2g39675) that was not represented among EST sequences. Each of these predicted target transcripts was validated as a miR173 target (Figure 1C).

Inspection of the four loci yielding miR173-targeted transcripts revealed that each was a confirmed or predicted ta-siRNA-generating locus (Figure 3). The three paralogous loci (At2g27400, At1g50055, and At2g39675) each contained sequences for the abundant siR255 and at least one siR255-related sequence (siR289, siR752, siR850, and siR438[+]) in a phased configuration (Figure 3). These ta-siRNAs were shown previously to be dependent on DCL1, RDR6, SGS3, and AGO1 and to target transcripts from the related genes At4g29760, At4g29770, and At5g18040 for degradation (Peragine et al., 2004; Vazquez et al., 2004b). This was consistent with expression profiling data in which At4g29770 was one of five genes that was upregulated in *dcl1-7*, *hen1-1*, and *rdr6-15* plants (Figure 2D). The three siRNA255-generating loci were designated *Trans-Acting siRNA1a* (*TAS1a*), *TAS1b*, and *TAS1c*. The fourth miR173 target locus, which mapped approximately 2 kb away from At2g39675 (Figure 3C), was antisense to the annotated sequence at At2g39680 and possessed the hallmarks of a ta-siRNA-generating site. Five phased small RNAs, such as the abundant siR1511 (Table S3), were identified from this locus (Figure 3C), and At2g39680-derived transcripts were upregulated in *dcl1-7*, *hen1-1*, and *rdr6-15* plants (Figure 2D). To confirm that At2g39680 is a ta-siRNA-generating locus, small RNAs from both polarities were analyzed using the miRNA- and siRNA-defective mutants. SiR1511, small RNAs detected using two antisense probes, and the control siR255 were each lost or diminished in *dcl1-7*, *hen1-1*, *hyl1-2*, *rdr6-11*, and *sgs3-11* but unaffected in *hst-15*, *dcl2-1*, *dcl3-1*, *rdr1-1*, and *rdr2-1* mutants (Figure 3E). We concluded that the At2g39680 locus, which was designated as *TAS2*, is an RDR6-dependent ta-siRNA-generating locus. A hypothetical ta-siRNA from the 3′D6(–) position (see below for position definition) at the *TAS2* locus (Figure 3C) was predicted to interact with at least two PPR gene transcripts (At1g12770 and At1g63130, Figure 3F), one of which was among the five *dcl1-1*, *hen1-1*, and *rdr6-15*-upregulated genes (Figure 2D). Target validation assays, however, failed to reveal a cleavage site at the predicted position within the transcript (Figure 3F).

The dependency of ta-siRNAs on RDR6/SGS3, and the nonoverlapping configuration of ta-siRNAs, suggests that ta-siRNA precursor or primary transcripts are converted to dsRNA forms and then processed by a DCL activity in phased, 21-nucleotide intervals. Setting the correct register for DCL-mediated cleavage must be a critical step in this pathway, as out-of-register processing would yield small RNAs with insufficient complementarity to their targets. We hypothesized that miR173-guided cleavage generates a defined terminus within a precursor transcript. After conversion of the precursor to dsRNA by RDR6/SGS3 activity, this terminus sets the register for successive DCL-mediated cleavage events in 21-nucleotide intervals. This hypothesis predicts that the predominant ta-siRNAs will form in a 21-nucleotide phase starting at the miR173 cleavage site. A position-dependent coding system was devised in which hypothetical DCL cleavage products from the miR173-targeted strand (3′D1[+], 3′D2[+], 3′D3[+], etc.) and opposite strand (3′D1[–], 3′D2[–], 3′D3[–], etc.) were designated relative to the miR173 target site (Figures 3A–3C).

Among the 25 unique small RNA sequences identified collectively in the ASRP database (Gustafson et al., 2005) and Vazquez et al. (Vazquez et al., 2004b) from all *TAS1* and *TAS2* loci, 16 sequences mapped precisely to the phasing interval set by miR173-guided cleavage (Figures 3A–3C). As predicted from the known properties of Dicer-like enzymes, siRNAs from the nontargeted strand (for example, siR143 and siR1946) were offset by two nucleotides relative to the complementary siRNA from the miR173 target strand. The register was maintained at each locus through at least the 3′D6 position and at *TAS1a* through the 3′D8 position. Twenty unique small RNAs, from positions 3′D1 to 3′D8, had 5′ ends formed by accurate in-phase cleavage but possessed 3′ ends offset by one nucleotide (data not shown). Two additional sequences had accurate 3′ ends but 5′ ends that were offset by one nucleotide (Vazquez et al., 2004b). Slight variation of this nature was expected based on the frequency of processing variants among *Arabidopsis* miRNA populations (Z.X., E.A., A. Calamar, and J.C.C., unpublished data).

miR390 Guides In-Phase Processing of *TAS3* ta-siRNA Primary Transcripts

The predicted miR390 target was a transcript from the annotated gene At3g17185 (Figure 4A), for which no function was assigned previously. The small hypothetical protein (50 amino acids) encoded by this gene contains no recognizable motifs, raising the possibility that At3g17185 is a misannotated, protein-noncoding locus.

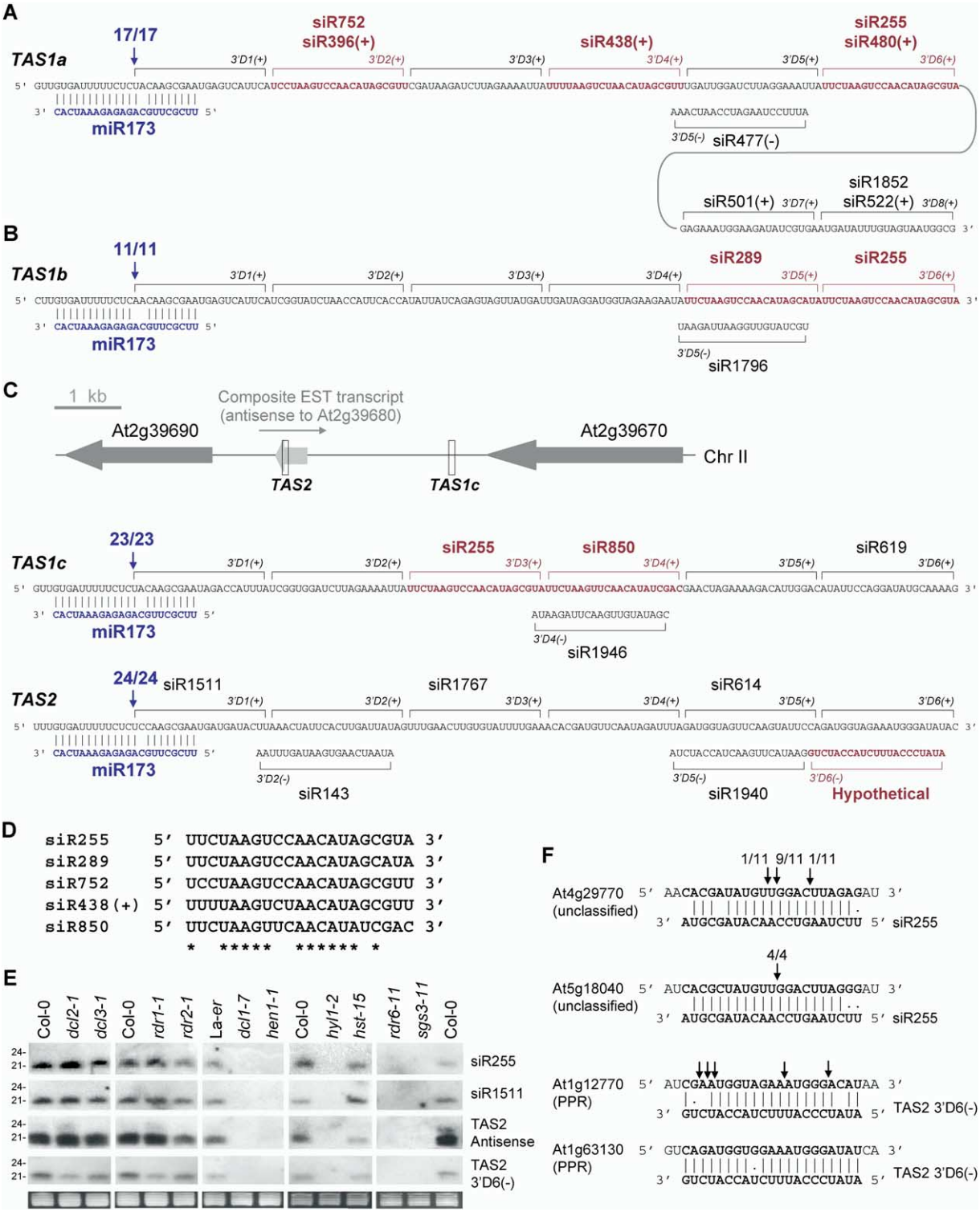

Figure 3. In-Phase Processing of ta-siRNAs Directed by miR173

(A–C) Diagrammatic representation of *TAS1a*, *TAS1b*, *TAS1c*, and *TAS2*. Predicted or validated ta-siRNAs are shown in red; all other cloned small RNA sequences are shown in black. siR480(+), siR396(+), siR438(+), siR477(–), siR501(+), and siR522(+) were from Vazquez et al. (2004b), and the remaining small RNAs were from the ASRP database (Gustafson et al., 2005; Xie et al., 2004). The 21-nucleotide phase relative to the miR173 cleavage site is indicated by brackets. The relative genomic positions of the *TAS1c* and *TAS2* loci are shown in (C).

(D) Alignment of siR255-like sequences.

(E) Ta-siRNA in miRNA- and siRNA-defective mutants. Small RNAs were detected using specific oligonucleotide probes, except *TAS2* antisense RNAs, which were detected using a transcript probe.

(F) Validation of siR255 target genes by 5′ RACE, and prediction of PPR transcripts targeted by a *TAS2* ta-siRNA from the 3′D6(–) position.

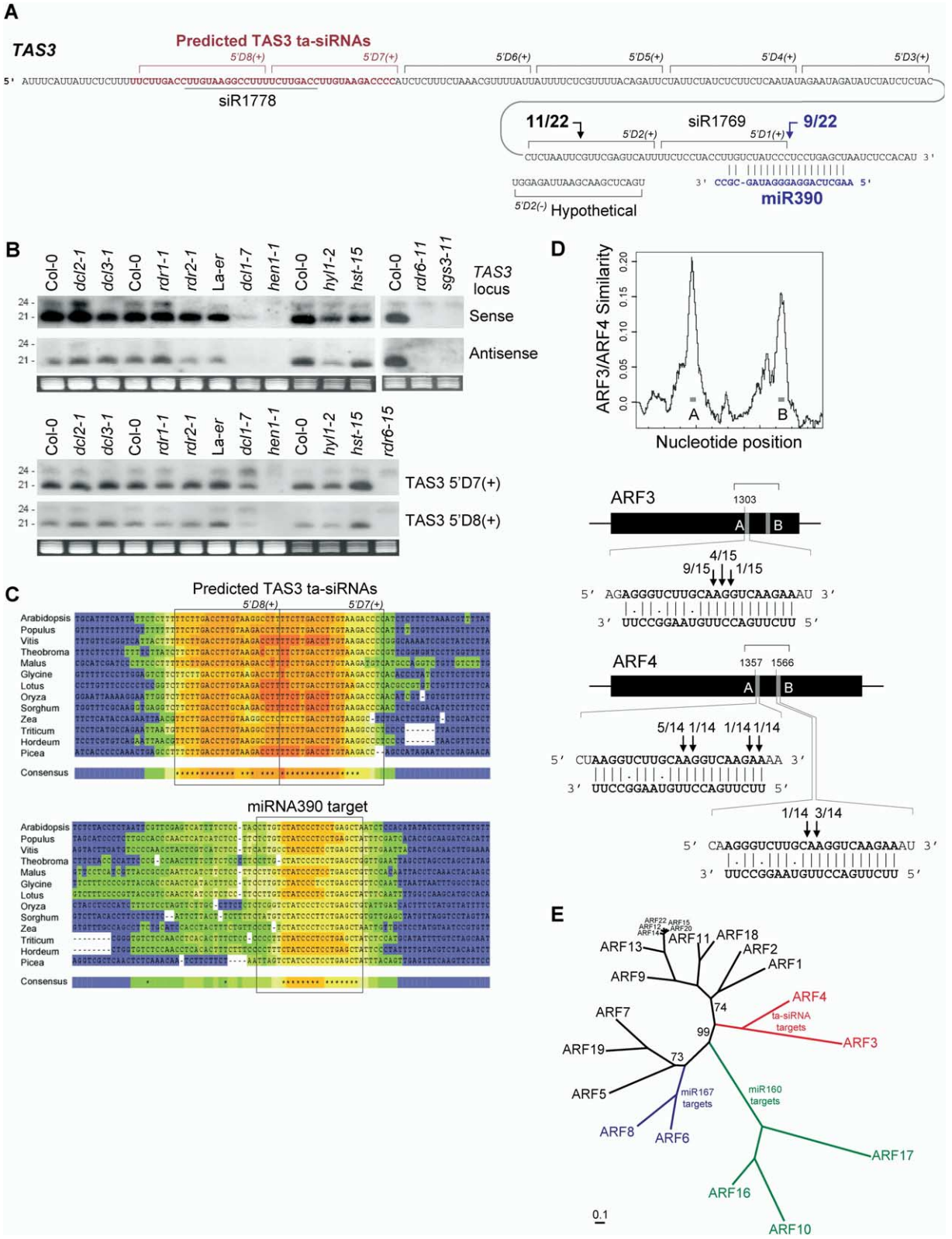

Figure 4. In-Phase Processing of *TAS3* ta-siRNAs Directed by miR390

(A) Diagrammatic representation of *TAS3* (At3g17185). The locus description codes are the same as in Figure 3, except that the ta-siRNAs derive from the 5′D1, 5′D2, 5′D3, etc. side of the miR390 cleavage site. Predicted functional ta-siRNAs are shown in red.

(B) Detection and validation of siRNAs from the sense and antisense (AS) strands corresponding to the 5′D11–5′D5 positions and the 5′D7(+) and 5′D8(+) positions.

The miR390 target site was validated by 5′RACE analysis (nine of 22 5′RACE products sequenced), although a second cleavage site 33 nucleotides away was detected at approximately the same frequency (11 of 22 5′RACE products; Figure 4A). Two low-abundance, cloned small RNAs (siR1769 and siR1778) were identified from sequences to the 5′ side of the miR390 cleavage (Figure 4A). In-phase, 21-nucleotide positions on the 5′ side of the miR390 cleavage site were coded as 5′D1(+), 5′D2(+), and so on (or 5′D1[–], 5′D2[–], etc. on the opposite strand). SiR1769 derived precisely from the 5′D1(+) position, whereas siR1778 was out of register (relative to the miR390-guided cleavage site) between the 5′D7(+) and 5′D8(+) positions.

The hypothesis that At3g17185 is a ta-siRNA-generating locus was tested first by blot assays of small RNAs and phylogenetic analysis. Transcript probes from sequences between the 5′D5 and the 5′D11 positions revealed DCL1-, HEN1-, RDR6-, and SGS3-dependent, 21-nucleotide small RNAs from both strands (Figure 4B, top panels). This locus also yielded low levels of 24-nucleotide RNAs, which were clearly DCL3 and RDR2 dependent but RDR6 and SGS3 independent (Figure 4B). Transcripts from each of 19 monocot or dicot species contained highly conserved miR390 target sites as well as a conserved set of tandemly arranged, near-identical 21-nucleotide segments that coaligned with the 5′D7(+) and 5′D8(+) positions (Figure 4C). The miR390 target site, 5′D7(+) sequence, and 5′D8(+) sequence represent conserved islands among nonconserved flanking sequences (Figure 4C). The phased spacing between the conserved, tandem sequences and the miR390 target site varied between the 5′D7(+)/5′D8(+) and the 5′D3(+)/5′D4(+) positions in different species. In all plants, however, the tandem sequences started in either perfect 21-nucleotide register (five of 19 species) or one-nucleotide offset (14 of 19 species) relative to the miR390 cleavage site (Figure 4 and data not shown). HEN1-, RDR6-, and DCL1-dependent, 21-nucleotide siRNAs were detected using probes corresponding to the conserved 5′D7(+) and 5′D8(+) positions (Figure 4B, bottom panel). The At3g17185 locus, therefore, was designated as *TAS3*.

Using the rules developed for miRNA target prediction, four genes (*ARF1*, *ARF2*, *ARF3*, and *ARF4*) were predicted as targets of these conserved, putative ta-siRNAs from the 5′D7(+) and 5′D8(+) positions of *TAS3*. *ARF3* and *ARF4* genes were upregulated in *dcl1-7*, *hen1-1*, and *rdr6-15* mutant plants (Figure 2D). Both *ARF3* and *ARF4* from 16 species contained two regions (A and B) of complementarity to the predicted *TAS3* ta-siRNAs (Figure 4D, and data not shown). The A site was also conserved in *ARF1* and *ARF2* genes in all plant species examined. The A site in both *ARF3* and *ARF4* was validated as a target site (Figure 4D). In contrast to most miRNA target sites, the *ARF3* and *ARF4* A sites yielded several minor cleavage products in addition to the major product formed by cleavage at the canonical target position (Figure 4D). Evidence supporting ta-siRNA targeting at the B site within the *ARF4* transcript was also obtained (Figure 4D).

Although a small RNA from the *TAS3* 5′D2(–) position was not cloned, a hypothetical ta-siRNA from this position may account for the second *TAS3* transcript cleavage site mapped by 5′RACE (Figure 4A). This site occurs precisely at the position predicted by cleavage guided by the 5′D2(–)-derived siRNA. This cleavage site is in precise 21-nucleotide register with siR1778. This suggests that siRNAs derived from ta-siRNA loci have the potential to interact with transcripts from which they originate.

MiRNA-Directed Biogenesis of ta-siRNAs in a Reconstruction System

To experimentally test the hypothesis that ta-siRNA biogenesis is initiated by miRNA-guided cleavage of primary transcripts, *TAS1* and *TAS2* were coexpressed transiently with *MIR173* in *Nicotiana benthamiana* leaves (Llave et al., 2002; Palatnik et al., 2003), and ta-siRNA accumulation was scored. Expression of full-length *TAS1b* (35S:TAS1b[+]), a short version of *TAS1b* (35S:TAS1b[+]sh), and full-length *TAS1a* (35S:TAS1a[+]) resulted in siR255 accumulation only in the presence of a construct (35S:miR173) expressing miR173 (Figure 5A, lanes 7, 8, 13, 14, 17, and 18). Likewise, siR255 from the *TAS1c* construct (35S:TAS1c[+]) and siR1511 from the *TAS2* construct (35S:TAS2[+]) both accumulated only in the presence of the miR173 construct (Figure 5B, lanes 7, 8, 11, and 12). Ta-siRNAs were not detected after expression of any of the *TAS1* or *TAS2* constructs alone (Figure 5A, lanes 3, 4, 11, 12, 15, and 16; Figure 5B, lanes 5, 6, 9, and 10) or after expression of the miR173-nontargeted strand of the short version of *TAS1b* (35S:TAS1b[–]sh) in either the presence or absence of miR173 (Figure 5A, lanes 5, 6, 9, and 10). In the presence of miR173, siR255 accumulated to levels up to 7.6-fold higher using the TAS1a(+) and TAS1c(+) constructs compared to the TAS1b(+) constructs. This may reflect a relatively poor miR173-TAS1b interaction, which involves two mismatched positions near the target cleavage site (Figure 3B).

To confirm that ta-siRNA biogenesis requires miRNA-directed targeting of primary transcripts, a *TAS1b* mutant construct (35S:TAS1b[+]shmut1) with a disrupted miR173 target site was expressed in the presence of miR173. The *TAS1b* mutant was also expressed in the presence of a modified miR173 construct (35S:miR173-res1) containing base substitutions to restore interac-

(C) Alignment of DNA sequences corresponding to the miR390 target site and *TAS3* ta-siRNAs in orthologs of 13 species. The quality of each aligned position was assessed using a scrolling window method, with best alignments coded in red and worst alignments in blue.
(D) Sequence similarity (PLOTCON, 21-nucleotide window) plots from alignment of an internal segment of 18 *ARF3* and *ARF4* genes from 16 species. Two highly conserved regions, indicated by "A" and "B," correspond to *TAS3* ta-siRNA target sites. Validation of ta-siRNA-directed cleavage of *ARF3* and *ARF4* target sites was by 5′RACE assays.
(E) Consensus phylogenetic tree of the *Arabidopsis* ARF gene family, showing miRNA and ta-siRNA regulated branches. Bayesian posterior probability was 100 except for nodes indicated otherwise.

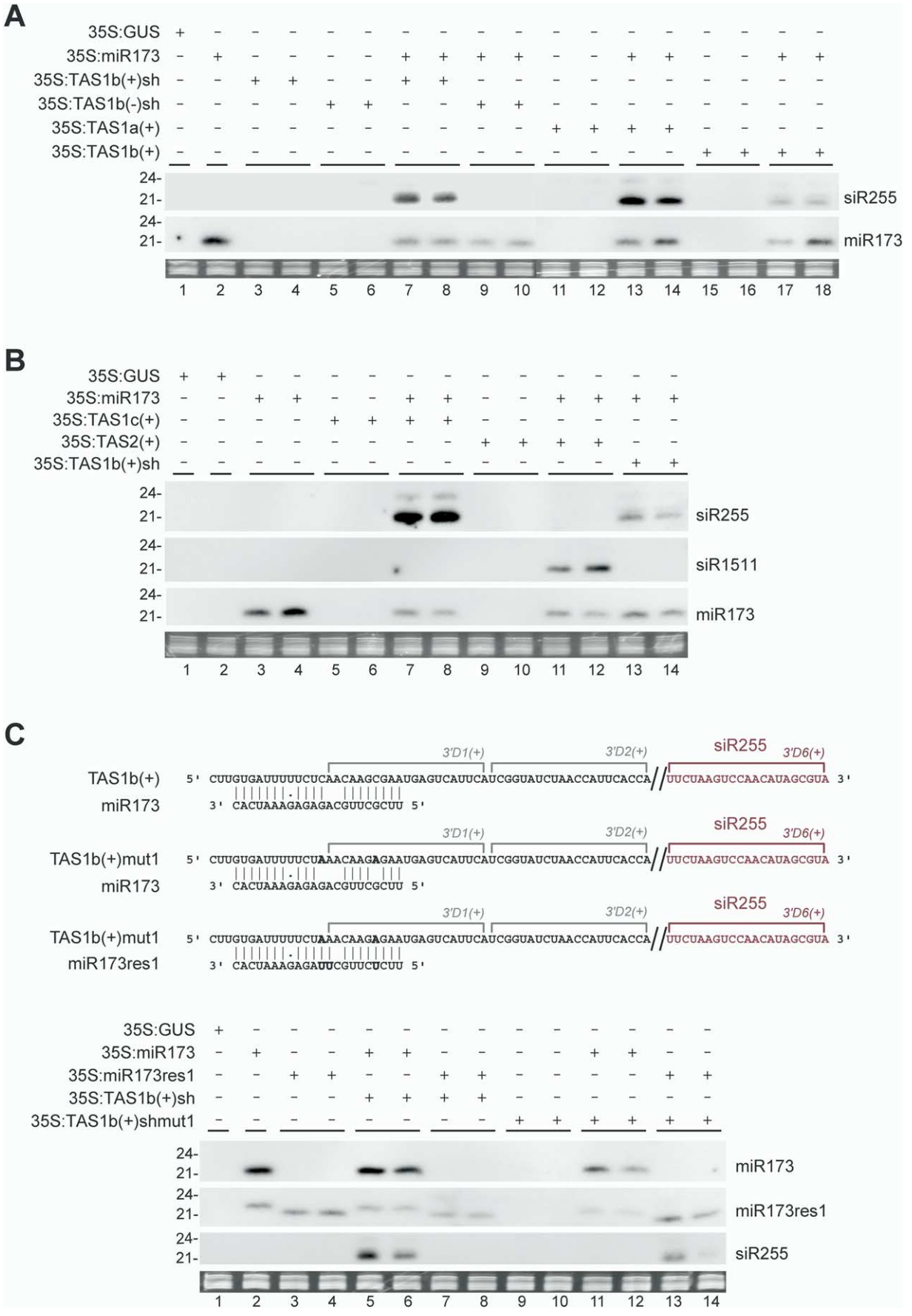
A
35S:GUS
35S:miR173
35S:TAS1b(+)sh
35S:TAS1b(-)sh
35S:TAS1a(+)
35S:TAS1b(+)
24-
21-
siR255
miR173
1 2 3 4 5 6 7 8 9 10 11 12 13 14 15 16 17 18
B
35S:GUS
35S:miR173
35S:TAS1c(+)
35S:TAS2(+)
35S:TAS1b(+)sh
siR255
siR1511
miR173
1 2 3 4 5 6 7 8 9 10 11 12 13 14
C
3'D1(+)
3'D2(+)
siR255
3'D6(+)
TAS1b(+)
miR173
TAS1b(+)mut1
miR173
TAS1b(+)mut1
miR173res1
35S:GUS
35S:miR173
35S:miR173res1
35S:TAS1b(+)sh
35S:TAS1b(+)shmut1
miR173
miR173res1
siR255
1 2 3 4 5 6 7 8 9 10 11 12 13 14

tion with the *TAS1b* mutant (Figure 5C, top). Mutations affecting the *TAS1b* target site or miR173 resulted in the loss of siR255 biogenesis (Figure 5C, lanes 7, 8, 11, and 12). In contrast, siR255 accumulation was restored when the *TAS1b* mutant was coexpressed with the miR173res1 construct (Figure 5C, lanes 13 and 14). These data clearly show that a functional miRNA target site in the ta-siRNA primary transcript is required to trigger ta-siRNA formation.

Discussion

Among several new *Arabidopsis* miRNA targets identified in this study, primary transcripts for ta-siRNA biogenesis were most surprising. The coincident register of miRNA-guided cleavage and phased Dicer-like processing of ta-siRNA precursors, combined with results of reconstruction experiments, support the hypothesis that miRNA targeting of primary transcripts sets the 21-nucleotide phase for accurate ta-siRNA formation. This explains why, for example, seven siR255 or related ta-siRNAs (siR850, siR289, siR752, and siR438[+]) from the three *TAS1* loci are all in phase relative to the respective miR173 target sites even though they originate from different positions between 3′D2(+) and 3′D6(+). Ta-siRNA primary transcript processing represents a new function for miRNAs and a departure from the canonical function of miRNAs as direct negative regulators. *MIR390* genes, miR390 target sites and ta-siRNAs in *TAS3* primary transcripts, and *TAS3* ta-siRNA target sites in *ARF3* and *ARF4* are all conserved between monocots and dicots, indicating this pathway is at least a few hundred million years old. The *MIR173* gene and its target sites are not similarly conserved and may have evolved relatively recently.

Exactly how does miRNA-guided cleavage lead to phased ta-siRNAs? We propose that RNA PolII transcripts from a ta-siRNA-generating locus are targeted for miRNA-guided cleavage at a position immediately to the 5′ or 3′ side of the ta-siRNA sequences (Figure 6, step 1). This is the initiation step required to route transcripts through the ta-siRNA biogenesis pathway. Recruitment of RDR6 polymerase to the cleaved precursor transcript (step 2) is proposed to occur by one of two routes. In the first, $RISC^{miRNA}$ or $RISC^{miRNA}$-associated factors may interact with RDR6 to deliver the polymerase to the transcript 3′ end (Hutvagner and Zamore, 2002). This might be analogous to recruitment of a viral RNA polymerase to the 3′ end of a template through interaction with proximal or distal template-associated factors (Kao et al., 2001). Alternatively, RDR6 may be recruited to transcripts due to aberrant features, such as the lack of a 5′ cap or 3′ polyadenylate tail (Gazzani et al., 2004). In any case, RDR6 is proposed to initiate transcription opposite a position at or near the 3′ end of the cleaved transcript. The role of SGS3, which appears to be required for RDR6-dependent reactions (Mourrain et al., 2000; Peragine et al., 2004; Vazquez et al., 2004b), is unclear. Using transcripts cleaved on the 5′ side of the ta-siRNA region (*TAS1* and *TAS2*), dsRNA formed by RDR6 polymerase activity extending to the template 5′ end would serve as the start point for end-dependent, sequential DCL-mediated cleavage reactions (step 3). For transcripts cleaved on the 3′ side (*TAS3*), duplex structure at the RDR6 polymerase initiation site would form the start point for subsequent DCL processing. Duplex ta-siRNAs from each round of cleavage are proposed to donate siRNAs into effector complexes (step 4) by mechanisms described for other siRNAs and miRNAs, as 76% of the cloned siRNAs from the five ta-siRNA-generating loci obey the strand asymmetry rules for RISC assembly (Khvorova et al., 2003; Schwarz et al., 2003). The activity of $RISC^{ta\text{-}siRNA}$ complexes on target mRNAs (or on ta-siRNA precursor transcripts; steps 5 and 6) likely occurs by AGO-dependent mechanisms, resulting in target cleavage and inactivation.

This model states that DCL-catalyzed processing of pre-ta-siRNA duplexes starts from ends that are defined by miRNA-guided cleavage. In principle, this seems reasonable as a phasing mechanism, although there are biochemical features of RDR6 and Dicer-like enzymes that should be considered. Both ends of the pre-ta-siRNA duplex are proposed to form through the activity of RDR6. Initiation and termination of synthesis at the extreme ends of a template would form blunt-ended dsRNA, which may be suboptimal as a DCL substrate relative to a substrate with two unpaired nucleotides at the 3′ end. However, primer-independent, RNA-dependent RNA polymerases of some viruses frequently initiate at sites inset from the template 3′ terminus, resulting in dsRNA products that contain 3′ nonpaired nucleotides (Kao et al., 2001). Some of these enzymes can also catalyze template-independent addition of nucleotides to the 3′ ends of product strands (Guan and Simon, 2000; Rao et al., 1989). It remains to be determined how RDR6 initiates and terminates on template RNAs and whether or not RDR6-catalyzed products are "optimized" DCL substrates.

What prevents siRNAs from the miRNA-nontargeted strands from guiding cleavage of ta-siRNA primary transcripts? Over 60% of the thermodynamically favored siRNA strands (Khvorova et al., 2003; Schwarz et al., 2003) from all theoretical positions within eight intervals from miRNA target sites at all ta-siRNA-generating loci occur in the miRNA-targeted strand, suggesting there may be selective pressure to minimize exposure of primary or precursor transcripts to secondary cleavage events. However, *TAS3* primary transcripts are likely cleaved by a RISC activity guided by the

Figure 5. Reconstruction of *TAS1a*, *TAS1b*, *TAS1c*, and *TAS2* ta-siRNA Biogenesis in a Transient Expression Assay using *N. benthamiana*

(A and B) Constructs with wild-type miR173 target sites. Constructs were expressed or coexpressed as indicated above the blot panels. The small RNAs detected in blot assays are shown to the right of each panel. Duplicate biological samples were analyzed for most treatments.
(C) Constructs with mutagenized target site or miR173 sequences. Target site and miRNA combinations tested are illustrated schematically above the blot panels. Mutagenized positions are in bold. The miR173res1 probe hybridized to both the miR173 and miR173res1 sequences.

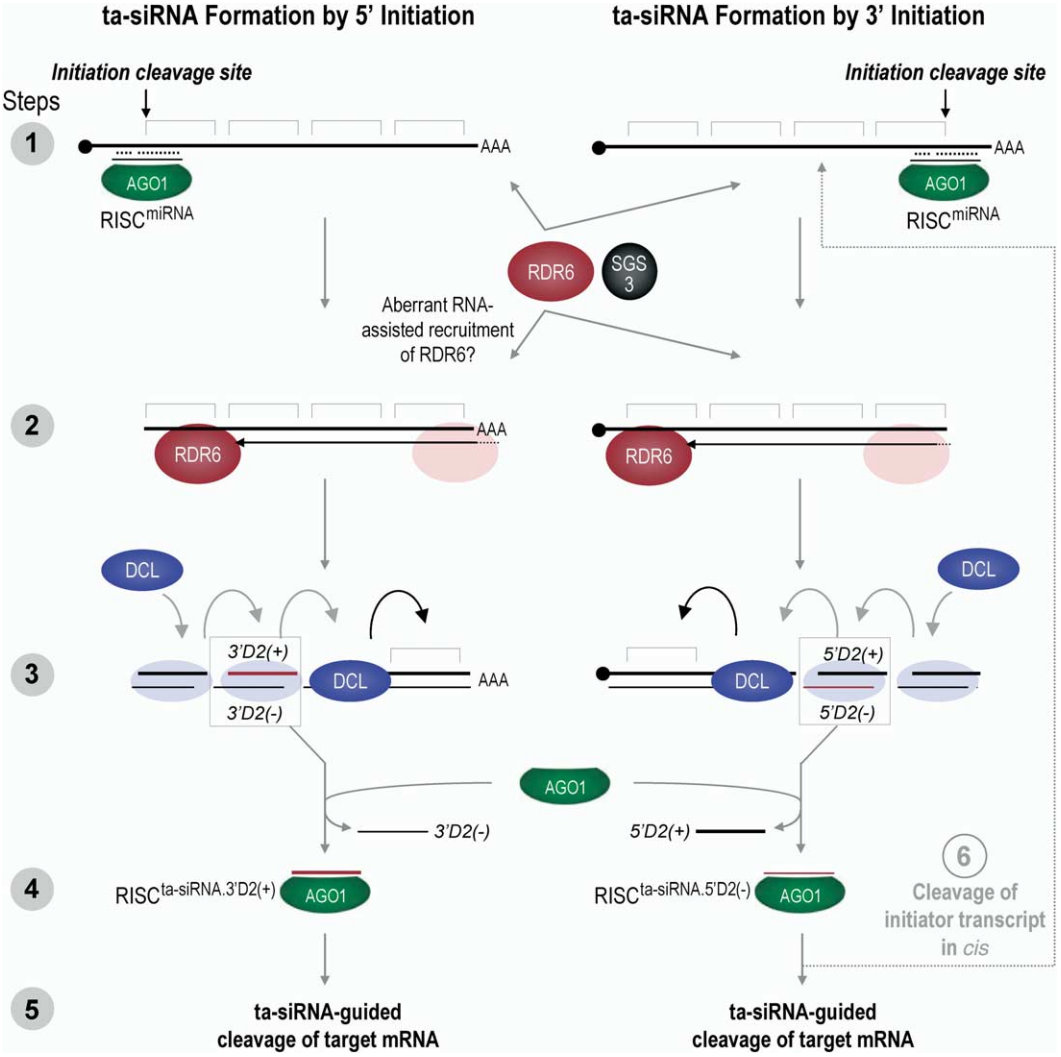

Figure 6. Model for miRNA-Directed Initiation of ta-siRNA Biogenesis

Brackets indicate a 21-nucleotide phase set by miRNA-guided cleavage. In step 3, hypothetical ta-siRNAs that incorporate into RISC are indicated in red.

5′D2(–) siRNA with an efficiency comparable to cleavage guided by miR390 (Figure 4A). Whether this is a regulatory mechanism to limit *TAS3* ta-siRNA formation or an inconsequential targeting event is not clear.

Finally, the finding that ARF3 and ARF4 transcripts are targeted by *TAS3* ta-siRNAs means that nearly one third of all ARF genes (23 known or predicted) are regulated by either miRNAs or ta-siRNAs (Figure 4E). ARF10, ARF16, and ARF17 are targets of miR160, while ARF6 and ARF8 are targets of miR167 (Jones-Rhoades and Bartel, 2004; Kasschau et al., 2003) (Figure 4E). The ARF proteins are transcription factors that transduce auxin signals during growth and development (Remington et al., 2004). ARF3, for example, functions in pattern specification in flowers (Nemhauser et al., 2000; Sessions et al., 1997). Interestingly, TIR1, an SCF-associated E3 ligase required for auxin signaling, is also under miRNA regulation (Jones-Rhoades and Bartel, 2004). The coupling of auxin and small RNA-based regulation suggests that miRNAs and ta-siRNAs confer a unique dimension to this signaling pathway. This might reflect a requirement for rapid clearance of auxin effector protein mRNAs immediately after signaling events (Bartel, 2004). Application of miRNAs as regulatory factors was also proposed as an evolutionary mechanism to confer regulatory diversity among members of multigene families (Allen et al., 2004). Data presented here suggest that regulatory diversity may be conferred by multiple small RNA pathways in plants.

Experimental Procedures

Small RNA Blots

Probes complementary to siR255 (TACGCTATGTTGGACTTAGAA) and siR1511 (AAGTATCATCATTCGCTTGGA) or LNA probes (Exiqon) to TAS3 5′D7(+) (TGGGGTCTTACAAGGTCAAGA), TAS3 5′D8(+) (AAAGGCCTTACAAGGTCAAGA), and TAS2 3′D6(–) (CAG ATGGTAGAAATGGGATAT) were end labeled with γ^{32}P-ATP using Optikinase (Amersham). T7 polymerase transcript probes corre-

sponding to At2g39680 5′D11–3′D11 and At3g17185 5′D11–5′D5 sequences were also generated. Low molecular weight RNA (5 μg) from *Arabidopsis* inflorescence tissue was isolated and subjected to blot assays as described (Allen et al., 2004).

Arabidopsis Mutants and Transgenes

Mutant lines for *dcl1-7*, *dcl2-1*, *dcl3-1*, *rdr1-1*, *rdr2-1*, *hen1-1*, *hyl1-2*, *rdr6-11*, *rdr6-15*, and *sgs3-11* were described previously (Allen et al., 2004; Park et al., 2002; Peragine et al., 2004; Vazquez et al., 2004a; Xie et al., 2004). The *hst-15* mutant (SALK_079290) contains a T-DNA insertion at position 1584 from the start codon (Alonso et al., 2003).

A genomic fragment (400 bp) surrounding the miR173 foldback was amplified and cloned (35S:miR173). A 400 bp fragment from *TAS1b* was amplified and cloned in both orientations in pMDC32, forming 35S:TAS1b(+)sh and 35S:TAS1b(–)sh. Mutations in 35S:miR173res1 and 35S:TAS1b(+)shmut1, as shown in Figure 5C, were generated by PCR and confirmed by sequencing. The 5′ and 3′ ends of primary transcripts for *TAS1a*, *TAS1b*, and *TAS1c* were inferred by 5′RACE assays and analysis of EST sequences. The ends for *TAS2* primary transcripts were inferred by 3′ cDNA cloning and analysis of and EST composite data (Table S1). Sequences corresponding to full-length transcripts from all *TAS1* and *TAS2* loci were amplified by PCR and cloned into pMDC32, forming 35S:TAS1a(+), 35S:TAS1b(+), 35S:TAS1c(+), and 35S:TAS2(+). *Agrobacterium*-mediated transfection assays in *N. benthamiana* leaves were done as described (Llave et al., 2002).

Microarray Analysis

Inflorescences (stages 1–12) from three plants per genotype comprised one replicate sample. All microarray analyses were done using three replicates. The control for *dcl1-1* and *hen1-1* mutants was La-*er*, and the control for *hyl1-2*, *hst-15*, *dcl2-1*, *dcl3-1*, *rdr1-1*, *rdr2-1*, and *rdr6-15* was Col-0. RNA was extracted using TRIzol reagent (Invitrogen) and purified using the Plant RNeasy Midi kit (Qiagen). Biotinylated complementary RNA (cRNA) was synthesized from 5 μg total RNA using the MessageAmp kit (Ambion). Concentration-adjusted cRNA (20 μg) was fragmented and hybridized to ATH1 GeneChip arrays (Affymetrix). Data were normalized using RMA Express (Bolstad et al., 2003) and analyzed using Genespring v7 (Silicon Genetics). Hierarchical clustering was done using standard clustering within GeneSpring.

Validation of miRNA and ta-siRNA Targets

Target validation was done using a 5′RACE assay as described (Kasschau et al., 2003; Llave et al., 2002). Gene-specific primers were designed approximately 500 nucleotides to the 3′ side of predicted target sites.

ARF Family Target Prediction and Phylogeny Reconstruction

Eighteen ARF3 and ARF4 sequences from 16 species were aligned using T-Coffee (Notredame et al., 2000). Similarity over a 21-nucleotide window was plotted using PLOTCON in the EMBOSS software suite (Rice et al., 2000). The ARF gene family phylogeny was analyzed by alignment of conserved ARF domain sequences using T-Coffee, followed by construction of a consensus family tree using a Bayesian method (Allen et al., 2004).

Supplemental Data

Supplemental Data include text, two figures, three tables, and Supplemental References and can be found with this article online at http://www.cell.com/cgi/content/full/121/2/207/DC1.

Acknowledgments

This work was supported by grants from the National Science Foundation (MCB-0209836), National Institutes of Health (AI43288), and USDA (2005-35319-15280). We thank Anne-Marie Girard for assistance with microarray experiments and Scott Givan, Chris Sullivan, and Daniel Smith for assistance and advice with computational resources. We thank Scott Poethig and Manabu Yoshikawa for generously providing seed and RNA for *rdr6-11* and *sgs3-11* mutants. We also thank lab members for advice and discussion.

Received: January 21, 2005
Revised: March 20, 2005
Accepted: April 5, 2005
Published: April 21, 2005

References

Achard, P., Herr, A., Baulcombe, D.C., and Harberd, N.P. (2004). Modulation of floral development by a gibberellin-regulated microRNA. Development *131*, 3357–3365.

Allen, E., Xie, Z., Gustafson, A.M., Sung, G.H., Spatafora, J.W., and Carrington, J.C. (2004). Evolution of microRNA genes by inverted duplication of target gene sequences in *Arabidopsis thaliana*. Nat. Genet. *36*, 1282–1290.

Alonso, J.M., Stepanova, A.N., Leisse, T.J., Kim, C.J., Chen, H., Shinn, P., Stevenson, D.K., Zimmerman, J., Barajas, P., Cheuk, R., et al. (2003). Genome-wide insertional mutagenesis of *Arabidopsis thaliana*. Science *301*, 653–657.

Ambros, V. (2003). MicroRNA pathways in flies and worms: growth, death, fat, stress, and timing. Cell *113*, 673–676.

Aukerman, M.J., and Sakai, H. (2003). Regulation of flowering time and floral organ identity by a microRNA and its APETALA2-like target genes. Plant Cell *15*, 2730–2741.

Bartel, D. (2004). MicroRNAs: genomics, biogenesis, mechanism, and function. Cell *116*, 281–297.

Bohnsack, M.T., Czaplinski, K., and Gorlich, D. (2004). Exportin 5 is a RanGTP-dependent dsRNA-binding protein that mediates nuclear export of pre-miRNAs. RNA *10*, 185–191.

Bollman, K.M., Aukerman, M.J., Park, M.Y., Hunter, C., Berardini, T.Z., and Poethig, R.S. (2003). HASTY, the *Arabidopsis* ortholog of exportin 5/MSN5, regulates phase change and morphogenesis. Development *130*, 1493–1504.

Bolstad, B.M., Irizarry, R.A., Astrand, M., and Speed, T.P. (2003). A comparison of normalization methods for high density oligonucleotide array data based on variance and bias. Bioinformatics *19*, 185–193.

Chan, S.W., Zilberman, D., Xie, Z., Johansen, L.K., Carrington, J.C., and Jacobsen, S.E. (2004). RNA silencing genes control de novo DNA methylation. Science *303*, 1336.

Chen, X. (2004). A microRNA as a translational repressor of APETALA2 in *Arabidopsis* flower development. Science *303*, 2022–2025.

Dalmay, T., Hamilton, A., Rudd, S., Angell, S., and Baulcombe, D.C. (2000). An RNA-dependent RNA polymerase gene in *Arabidopsis* is required for posttranscriptional gene silencing mediated by a transgene but not by a virus. Cell *101*, 543–553.

Emery, J.F., Floyd, S.K., Alvarez, J., Eshed, Y., Hawker, N.P., Izhaki, A., Baum, S.F., and Bowman, J.L. (2003). Radial patterning of *Arabidopsis* shoots by class III HD-ZIP and KANADI genes. Curr. Biol. *13*, 1768–1774.

Fagard, M., Boutet, S., Morel, J., Bellini, C., and Vaucheret, H. (2000). AGO1, QDE-2, and RDE-1 are related proteins required for post-transcriptional gene silencing in plants, quelling in fungi and RNA interference in animals. Proc. Natl. Acad. Sci. USA *97*, 11650–11654.

Gazzani, S., Lawrenson, T., Woodward, C., Headon, D., and Sablowski, R. (2004). A link between mRNA turnover and RNA interference in *Arabidopsis*. Science *306*, 1046–1048.

Guan, H., and Simon, A.E. (2000). Polymerization of nontemplate bases before transcription initiation at the 3′ ends of templates by an RNA-dependent RNA polymerase: an activity involved in 3′ end repair of viral RNAs. Proc. Natl. Acad. Sci. USA *97*, 12451–12456.

Gustafson, A.M., Allen, E., Givan, S., Smith, D., Carrington, J.C., and Kasschau, K.D. (2005). ASRP: the *Arabidopsis* Small RNA Project Database. Nucleic Acids Res. *33*, D637–D640.

Han, M.H., Goud, S., Song, L., and Fedoroff, N. (2004). The *Arabi-*

dopsis double-stranded RNA-binding protein HYL1 plays a role in microRNA-mediated gene regulation. Proc. Natl. Acad. Sci. USA *101*, 1093–1098.

He, L., and Hannon, G.J. (2004). MicroRNAs: small RNAs with a big role in gene regulation. Nat. Rev. Genet. *5*, 522–531.

Hutvagner, G., and Zamore, P.D. (2002). RNAi: nature abhors a double-strand. Curr. Opin. Genet. Dev. *12*, 225–232.

Jones-Rhoades, M.W., and Bartel, D.P. (2004). Computational identification of plant microRNAs and their targets, including a stress-induced miRNA. Mol. Cell *14*, 787–799.

Juarez, M.T., Kui, J.S., Thomas, J., Heller, B.A., and Timmermans, M.C. (2004). microRNA-mediated repression of rolled leaf1 specifies maize leaf polarity. Nature *428*, 84–88.

Kao, C.C., Singh, P., and Ecker, D.J. (2001). De novo initiation of viral RNA-dependent RNA synthesis. Virology *287*, 251–260.

Kasschau, K.D., Xie, Z., Allen, E., Llave, C., Chapman, E.J., Krizan, K.A., and Carrington, J.C. (2003). P1/HC-Pro, a viral suppressor of RNA silencing, interferes with *Arabidopsis* development and miRNA function. Dev. Cell *4*, 205–217.

Khvorova, A., Reynolds, A., and Jayasena, S.D. (2003). Functional siRNAs and miRNAs exhibit strand bias. Cell *115*, 209–216.

Kidner, C.A., and Martienssen, R.A. (2004). Spatially restricted microRNA directs leaf polarity through ARGONAUTE1. Nature *428*, 81–84.

Kurihara, Y., and Watanabe, Y. (2004). *Arabidopsis* micro-RNA biogenesis through Dicer-like 1 protein functions. Proc. Natl. Acad. Sci. USA *101*, 12753–12758.

Lappartient, A.G., Vidmar, J.J., Leustek, T., Glass, A.D., and Touraine, B. (1999). Inter-organ signaling in plants: regulation of ATP sulfurylase and sulfate transporter genes expression in roots mediated by phloem-translocated compound. Plant J. *18*, 89–95.

Laufs, P., Peaucelle, A., Morin, H., and Traas, J. (2004). MicroRNA regulation of the CUC genes is required for boundary size control in *Arabidopsis* meristems. Development *131*, 4311–4322.

Liu, Q., Rand, T.A., Kalidas, S., Du, F., Kim, H.E., Smith, D.P., and Wang, X. (2003). R2D2, a bridge between the initiation and effector steps of the *Drosophila* RNAi pathway. Science *301*, 1921–1925.

Liu, J., Carmell, M.A., Rivas, F.V., Marsden, C.G., Thomson, J.M., Song, J.J., Hammond, S.M., Joshua-Tor, L., and Hannon, G.J. (2004). Argonaute2 is the catalytic engine of mammalian RNAi. Science *305*, 1437–1441.

Llave, C., Xie, Z., Kasschau, K.D., and Carrington, J.C. (2002). Cleavage of Scarecrow-like mRNA targets directed by a class of *Arabidopsis* miRNA. Science *297*, 2053–2056.

Lund, E., Guttinger, S., Calado, A., Dahlberg, J.E., and Kutay, U. (2003). Nuclear export of microRNA precursors. Science *303*, 95–98.

Mallory, A.C., Dugas, D.V., Bartel, D.P., and Bartel, B. (2004). MicroRNA regulation of NAC-domain targets is required for proper formation and separation of adjacent embryonic, vegetative, and floral organs. Curr. Biol. *14*, 1035–1046.

Meister, G., Landthaler, M., Patkaniowska, A., Dorsett, Y., Teng, G., and Tuschl, T. (2004). Human Argonaute2 mediates RNA cleavage targeted by miRNAs and siRNAs. Mol. Cell *15*, 185–197.

Mourrain, P., Beclin, C., Elmayan, T., Feuerbach, F., Godon, C., Morel, J.B., Jouette, D., Lacombe, A.M., Nikic, S., Picault, N., et al. (2000). *Arabidopsis* SGS2 and SGS3 genes are required for post-transcriptional gene silencing and natural virus resistance. Cell *101*, 533–542.

Nemhauser, J.L., Feldman, L.J., and Zambryski, P.C. (2000). Auxin and ETTIN in *Arabidopsis* gynoecium morphogenesis. Development *127*, 3877–3888.

Notredame, C., Higgins, D.G., and Heringa, J. (2000). T-Coffee: a novel method for fast and accurate multiple sequence alignment. J. Mol. Biol. *302*, 205–217.

Olsen, P.H., and Ambros, V. (1999). The lin-4 regulatory RNA controls developmental timing in *Caenorhabditis elegans* by blocking LIN-14 protein synthesis after the initiation of translation. Dev. Biol. *216*, 671–680.

Palatnik, J.F., Allen, E., Wu, X., Schommer, C., Schwab, R., Carrington, J.C., and Weigel, D. (2003). Control of leaf morphogenesis by microRNAs. Nature *425*, 257–263.

Parizotto, E.A., Dunoyer, P., Rahm, N., Himber, C., and Voinnet, O. (2004). In vivo investigation of the transcription, processing, endonucleolytic activity, and functional relevance of the spatial distribution of a plant miRNA. Genes Dev. *18*, 2237–2242.

Park, W., Li, J., Song, R., Messing, J., and Chen, X. (2002). CARPEL FACTORY, a Dicer homolog, and HEN1, a novel protein, act in microRNA metabolism in *Arabidopsis thaliana*. Curr. Biol. *12*, 1484–1495.

Park, M.Y., Wu, G., Gonzalez-Sulser, A., Vaucheret, H., and Poethig, R.S. (2005). Nuclear processing and export of microRNAs in Arabidopsis. Proc. Natl. Acad. Sci. USA *102*, 3691–3696.

Peragine, A., Yoshikawa, M., Wu, G., Albrecht, H.L., and Poethig, R.S. (2004). SGS3 and SGS2/SDE1/RDR6 are required for juvenile development and the production of trans-acting siRNAs in *Arabidopsis*. Genes Dev. *18*, 2368–2379.

Pham, J.W., Pellino, J.L., Lee, Y.S., Carthew, R.W., and Sontheimer, E.J. (2004). A Dicer-2-dependent 80S complex cleaves targeted mRNAs during RNAi in *Drosophila*. Cell *117*, 83–94.

Rao, A.L., Dreher, T.W., Marsh, L.E., and Hall, T.C. (1989). Telomeric function of the tRNA-like structure of brome mosaic virus RNA. Proc. Natl. Acad. Sci. USA *86*, 5335–5339.

Reinhart, B.J., Weinstein, E.G., Rhoades, M.W., Bartel, B., and Bartel, D.P. (2002). MicroRNAs in plants. Genes Dev. *16*, 1616–1626.

Remington, D.L., Vision, T.J., Guilfoyle, T.J., and Reed, J.W. (2004). Contrasting modes of diversification in the Aux/IAA and ARF gene families. Plant Physiol. *135*, 1738–1752.

Rhoades, M.W., Reinhart, B.J., Lim, L.P., Burge, C.B., Bartel, B., and Bartel, D.P. (2002). Prediction of plant microRNA targets. Cell *110*, 513–520.

Rice, P., Longden, I., and Bleasby, A. (2000). EMBOSS: the European Molecular Biology Open Software Suite. Trends Genet. *16*, 276–277.

Schauer, S.E., Jacobsen, S.E., Meinke, D.W., and Ray, A. (2002). *DICER-LIKE1*: blind men and elephants in *Arabidopsis* development. Trends Plant Sci. *7*, 487–491.

Schwarz, D.S., Hutvagner, G., Du, T., Xu, Z., Aronin, N., and Zamore, P.D. (2003). Asymmetry in the assembly of the RNAi enzyme complex. Cell *115*, 199–208.

Seggerson, K., Tang, L., and Moss, E.G. (2002). Two genetic circuits repress the *Caenorhabditis elegans* heterochronic gene *lin-28* after translation initiation. Dev. Biol. *243*, 215–225.

Sessions, A., Nemhauser, J.L., McColl, A., Roe, J.L., Feldmann, K.A., and Zambryski, P.C. (1997). ETTIN patterns the *Arabidopsis* floral meristem and reproductive organs. Development *124*, 4481–4491.

Sunkar, R., and Zhu, J.K. (2004). Novel and stress-regulated microRNAs and other small RNAs from *Arabidopsis*. Plant Cell *16*, 2001–2019.

Tang, G., Reinhart, B.J., Bartel, D.P., and Zamore, P.D. (2003). A biochemical framework for RNA silencing in plants. Genes Dev. *17*, 49–63.

Tomari, Y., Matranga, C., Haley, B., Martinez, N., and Zamore, P.D. (2004). A protein sensor for siRNA asymmetry. Science *306*, 1377–1380.

Vaucheret, H., Vazquez, F., Crete, P., and Bartel, D.P. (2004). The action of ARGONAUTE1 in the miRNA pathway and its regulation by the miRNA pathway are crucial for plant development. Genes Dev. *18*, 1187–1197.

Vazquez, F., Gasciolli, V., Crete, P., and Vaucheret, H. (2004a). The nuclear dsRNA binding protein HYL1 is required for microRNA accumulation and plant development, but not posttranscriptional transgene silencing. Curr. Biol. *14*, 346–351.

Vazquez, F., Vaucheret, H., Rajagopalan, R., Lepers, C., Gasciolli, V., Mallory, A.C., Hilbert, J.L., Bartel, D.P., and Crete, P. (2004b). Endogenous trans-acting siRNAs regulate the accumulation of *Arabidopsis* mRNAs. Mol. Cell *16*, 69–79.

Xie, Z., Kasschau, K.D., and Carrington, J.C. (2003). Negative feedback regulation of Dicer-Like1 in *Arabidopsis* by microRNA-guided mRNA degradation. Curr. Biol. *13*, 784–789.

Xie, Z., Johansen, L.K., Gustafson, A.M., Kasschau, K.D., Lellis, A.D., Zilberman, D., Jacobsen, S.E., and Carrington, J.C. (2004). Genetic and functional diversification of small RNA pathways in plants. PLoS Biol. *2*, 642–652.

Yi, R., Qin, Y., Macara, I.G., and Cullen, B.R. (2003). Exportin-5 mediates the nuclear export of pre-microRNAs and short hairpin RNAs. Genes Dev. *17*, 3011–3016.

Yu, D., Fan, B., MacFarlane, S.A., and Chen, Z. (2003). Analysis of the involvement of an inducible *Arabidopsis* RNA-dependent RNA polymerase in antiviral defense. Mol. Plant Microbe Interact. *16*, 206–216.

Yu, B., Yang, Z., Li, J., Minakhina, S., Yang, M., Padgett, R.W., Steward, R., and Chen, X. (2005). Methylation as a crucial step in plant microRNA biogenesis. Science *307*, 932–935.

Zilberman, D., Cao, X., and Jacobsen, S.E. (2003). ARGONAUTE4 control of locus-specific siRNA accumulation and DNA and histone methylation. Science *299*, 716–719.

Accession Numbers

Microarray data were deposited in the NCBI Gene Expression Omnibus (http://www.ncbi.nlm.nih.gov/geo/) under accession number GSE2473.